Macromolecules **1981**, *14*, 1567–1575

(5) Olabisi, O.; Robeson, L. M.; Shaw, M. T. "Polymer-Polymer Miscibility"; Academic Press: New York, 1979.
(6) Birks, J. B. "Photophysics of Aromatic Molecules"; Wiley: New York, 1970.
(7) Förster, Th. *Proc. Faraday Soc.* **1959**, *27*, 7.
(8) Berlman, I. B. "Energy Transfer Parameters of Aromatic Compounds"; Academic Press: New York, 1973.
(9) Klöpffer, W. *Ann. N.Y. Acad. Sci.* **1981**, *366*, 373–86.
(10) Frank, C. W.; Gashgari, M. A. *Macromolecules* **1979**, *12*, 163.
(11) Frank, C. W.; Gashgari, M. A.; Chutikamontham, P.; Haverly, V. In "Structure and Properties of Amorphous Polymers"; Walton, A. G., Ed.; Elsevier: Amsterdam, 1980; pp 187–210.
(12) Semerak, S. N.; Frank, C. W. *Macromolecules* **1981**, *14*, 443–9.
(13) Frank, C. W.; Harrah, L. A. *J. Chem. Phys.* **1974**, *61*, 1526.
(14) Frank, C. W.; Gashgari, M. A. *Ann. N.Y. Acad. Sci.* **1981**, *366*, 387–403.
(15) Demeyer, K.; van der Auwerger, M.; Aerts, L.; De Schryver, F. C. *J. Chim. Phys.* **1980**, *77*, 493.
(16) Webber, S. E.; Avots-Avotins, P. E.; Deumié, M. *Macromolecules* **1981**, *14*, 105.
(17) Holden, D. A.; Wang, P. Y. K.; Guillet, J. E. *Macromolecules* **1980**, *13*, 295.
(18) Gelles, R. G.; Frank, C. W., manuscript in preparation.
(19) Hildebrand, J. H.; Scott, R. L. "Regular Solutions"; Prentice-Hall: New York, 1962.
(20) Krause, S. *J. Macromol. Sci., Rev. Macromol. Chem.* **1972**, *C7*, 251.
(21) Krause, S., Chapter 2 of ref 4.
(22) Flory, P. J. *J. Chem. Phys.* **1941**, *9*, 660.
(23) Flory, P. J. *J. Chem. Phys.* **1942**, *10*, 51.
(24) Huggins, M. L. *J. Chem. Phys.* **1941**, *9*, 440.
(25) Huggins, M. L. *Ann. N.Y. Acad. Sci.* **1942**, *43*, 1.
(26) Tompa, H. "Polymer Solutions"; Butterworths: London, 1956.
(27) Koningsveld, R. Ph.D. Thesis, University of Leiden, 1967.
(28) Prigogine, I. "The Molecular Theory of Solutions"; North-Holland Publishing Co., Amsterdam, and Interscience, New York, 1957; Chapters 11, 17.
(29) Huggins, M. L. *J. Phys. Chem.* **1970**, *74*, 371.
(30) Huggins, M. L. *J. Phys. Chem.* **1971**, *75*, 1255.
(31) Huggins, M. L. *MTP Int. Rev. Sci., Phys. Chem., Ser. 2* **1974**, *8*, 123.
(32) Koningsveld, R.; Kleintjens, L. A. *J. Polym. Sci., Polym. Symp.* **1977**, *61*, 221.
(33) Flory, P. J.; Orwoll, R. A.; Vrij, A. *J. Am. Chem. Soc.* **1964**, *86*, 3515.
(34) Flory, P. J. *J. Am. Chem. Soc.* **1965**, *87*, 1833.
(35) McMaster, L. P. *Macromolecules* **1973**, *6*, 760.
(36) Biros, J.; Zeman, L.; Patterson, D. *Macromolecules* **1971**, *4*, 30.
(37) Lewis, O. G. "Physical Constants of Linear Homopolymers"; Springer-Verlag: New York, 1968.
(38) Scott, R. L. *J. Chem. Phys.* **1949**, *17*, 279.
(39) Bueche, F. "Physical Properties of Polymers"; Wiley: New York, 1962.

Equation of State of Pressure-Densified Glasses of Poly(vinyl chloride)

Motosuke Naoki,* Hirotoshi Mori, and Akira Owada

Department of Textiles and Polymers, Faculty of Technology, Gunma University, Tenjin-cho, Kiryu-shi, Gunma 376, Japan. *Received November 7, 1980*

ABSTRACT: Volumetric data of poly(vinyl chloride) glasses formed from the liquid state by isobaric cooling at a constant rate under pressures of 1, 150, 300, and 500 kg cm^{-2} are reported. The pressure–volume–temperature relations of the glasses are shown to be described with the principle of corresponding states. The characteristic volume and entropy are not affected by the pressure densification, while the characteristic temperature, pressure, and internal energy increase with increasing glass-forming pressure. Some theoretical equations of state for polymer liquids are applied to the glasses, but they are in serious disagreement with the experiments. Also discussed is an equation of state derived from cell theory by introducing a distribution of the cell size in its simplest form, which gives results quite close to the experimental *PVT* data and the internal energy. The presented results suggest that the localized energy field may play an important role in the molecular motions and the configurational properties of the glass.

I. Introduction

It is well-known that the density of a glass depends on its thermodynamic history. Many investigators have shown that formation of organic,[1,2] inorganic oxide,[3] and polymer[2,4-13] glasses by lowering the temperature at elevated pressures leads to samples which are more dense. Effects of pressure densification on the pressure–volume–temperature (*PVT*) relations of the glasses were first studied by McKinney and Goldstein,[12] who obtained *PVT* data for two glasses of poly(vinyl acetate) (PVAc) by using the same isobaric cooling rate at 1 and 800 bars. The *PVT* surfaces of the pressure-densified glasses are illustrated schematically in Figure 1.

The liquid and various glass surfaces are continuous only through their respective glass transition intersection line, the $T_g(P)$ line in Figure 1. The $T_g(P)$ line approximately corresponds to the isorelaxation time line on which a mean volume relaxation time is essentially constant as pressure is varied.[14-16] The intersection line of the liquid and P_0 glass surface is shown as the iso-free-volume line in Figure 1. Similar lines are available for the other glasses. If the glass transition is determined in terms of one ordering parameter, e.g., the free volume, the iso-free-volume lines should be identical with the $T_g(P)$ line. This is, in fact, not realized,[12] as illustrated in Figure 1. Therefore, the glassy state cannot be described in terms of a single ordering parameter.

Theoretical approaches to the equation of state of polymer glasses have been demonstrated by Somcynsky and Simha[17] and Nose,[18] who employed hole theory. In their treatments, the glass is viewed as the state where the rearrangements of holes are forbidden. Below the glass transition temperature, their hole theories become equivalent to traditional cell theories.[19,20] However, Quach and Simha[21] showed that the assumption of a constant hole fraction in the glassy state was an oversimplification. Later McKinney and Simha[22] introduced a notion of gradual freeze-in of the hole fraction, treated the hole fraction as an adjustable, pressure- and temperature-dependent parameter to be obtained by experiment, and analyzed the *PVT* data of PVAc glasses.[12] They deduced that the partial freeze-in of the hole fraction was due to a size distribution of hole clusters.

The purpose of this paper is first to give detailed *PVT* data of the pressure-densified glasses of poly(vinyl chloride) (PVC), second to elucidate the correspondence among

0024-9297/81/2214-1567$01.25/0 © 1981 American Chemical Society

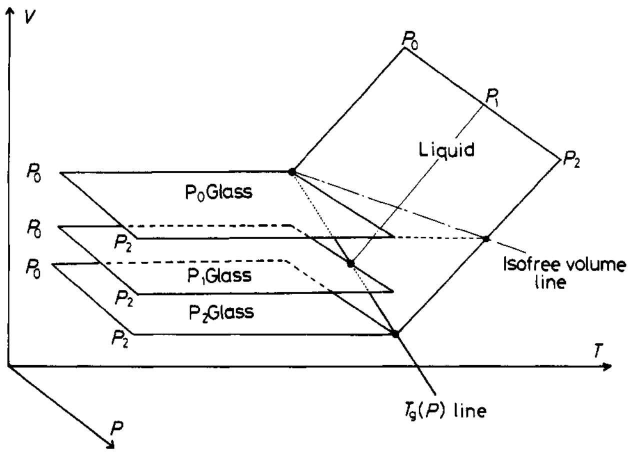

Figure 1. Schematic diagram illustrating liquid and glass surfaces in the *PVT* space. P_0, P_1, and P_2 glass are the glasses formed at a constant cooling rate under the pressures P_0, P_1, and P_2.

them (section IV), and third to discuss the equation of state of the glasses (section V). In section VI, a modified cell theory which represents the *PVT* data of the glasses is proposed.

II. Experimental Section

Sample. All measurements were made on a single sample of PVC supplied by Toyo Soda Co. The number-average molecular weight was 44 000. After being purified by swelling with tetrahydrofuran and deswelling with methanol, the PVC sample in fine fibrous form was dried for 1 week in a vacuum oven at 60 °C. Then 0.4-mm-thick sheets were molded in a vacuum press under 350 kg cm^{-2} at 150 °C.

A cylindrical glass tube in which the sample was placed was evacuated and brought up to 100 °C. After being kept there for 30 min, the temperature was lowered to −35 °C at a cooling rate of 0.24 K/min. Thus-prepared glass is referred to as 0 glass. A reference value of the specific volume for 0 glass was determined by the floating method at 45 °C, using a mixture of calcium chloride and water.

The densification procedure is as follows. The PVC sample in the dilatometer illustrated in Figure 2 was heated under atmospheric pressure to a temperature T_x which was higher than the glass transition temperature $T_g(P_x)$ by about 25 K. The pressure was then increased to the glass-forming pressure P_x. After the pressure and temperature were kept at P_x and T_x for 30 min, the system was isobarically cooled to −35 °C at a rate of 0.24 K/min. The thus-prepared densified glasses under 150, 300, and 500 kg cm^{-2} are referred to as 150 glass, 300 glass, and 50 glass, respectively.

Bulk PVC has been regarded to have a small fraction of crystalline content (typically 5–12%),[23] but there have been various interpretations on the nature of the crystalline content and the extent of crystallinity.[24] From small-angle X-ray scattering (SAXS) studies, Straff and Uhlmann showed that even if all the heterogeneities indicated by their SAXS data on PVC were crystallites, the crystallinity would be only about 0.5%.[24c] Since it seems quite difficult to obtain a reliable value of crystallinity for the respective PVC sample, we assume that the crystallinity of the glasses does not vary with pressure and temperature over the present experimental range.

Equipment. The densifications and the measurements of the *PVT* relations were carried out in a dilatometer set in a pressure vessel which was immersed in a bath controlled to an accuracy of ±0.02 K. In the pressure vessel, the temperature was controlled within ±0.004 K. A diagram of the pressure dilatometer is shown in Figure 2. Silicone oil (KF-94, Shin-Etsu Chemical Co.) was used to transmit the hydrostatic pressure. The pressure was measured by a Heise bourdon gauge with an automatic compensator (Dresser Industries) and the temperature by an alumel–chromel thermocouple (6) inserted in the pressure cell.

Changes in the mercury level of the Pyrex dilatometer (1) were read by measuring the emf of a variable transformer (1501-9, Shinko Electric Co.) (5) induced by a piece of Permalloy (4) set on the top of mercury column (3). The *PVT* data for mercury taken from ref 25 and 26 and a mercury-filled dilatometer were used to calibrate the emf of the transformer and to calculate the specific volume of the sample. Variations of the emf with pressure were negligibly small up to 1000 kg cm^{-2} but those with temperature were not; e.g., the emf increased about 10% when the temperature was raised from 0 to 50 °C.

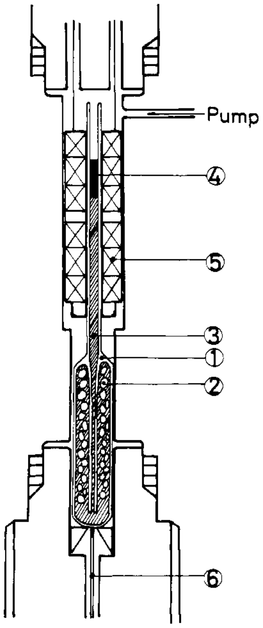

Figure 2. Diagram of pressure dilatometer: (1) dilatometer made of Pyrex glass; (2) sample; (3) mercury; (4) Permalloy; (5) variable differential transformer; (6) alumel–chromel thermocouple.

Operation. Isothermal experiments were carried out to give the *PVT* relations of the 0, 150, 300, and 500 glasses at 10 K intervals over a temperature range of 250–340 K. The pressure was changed in increments of 50 kg cm^{-2} in the 1–200 kg cm^{-2} region and in increments of 100 kg, cm^{-2} in the 200–600 kg cm^{-2} region. After completion of the isothermal experiments, the atmospheric V–T relations of all the glasses were measured at 1 K intervals with a continuous heating rate of 0.24 K/min from 240 to 360 K.

The specific volume of the sample at temperature T and pressure P_j was calculated from

$$w_s V_s(T,P_j) = [w_s V_s(T,P_{j-1}) + w_{\mathrm{Hg}} V_{\mathrm{Hg}}(T,P_{j-1})] \times [1 - \beta_{P_j}(P_j - P_{j-1})] - w_{\mathrm{Hg}} V_{\mathrm{Hg}}(T,P_j) + \Delta V_{j,\mathrm{measd}} + \Delta V_{j,\Delta P} \quad \text{(II-1)}$$

where w_s and w_{Hg} were the weights of the sample and the mercury loaded in the dilatometer, V_s and V_{Hg} were the specific volumes of the sample and the mercury, β_{P_j} was the compressibility of the dilatometer at P_j, $\Delta V_{j,\mathrm{measd}}$ was the volume change of the sample and the mercury as the pressure was increased from P_{j-1} to P_j, and $\Delta V_{j,\Delta P}$ was the correction due to the change in the length of the transformer with the pressure increment. The thermal expansitivity, α_p, and the compressibility, β_p, of the dilatometer used in the present study were expressed as

$$\alpha_p = \alpha_1 - bP - (d/2)P^2 \quad \text{(II-2)}$$

$$\beta_p = (a + bT) + (c + dT)P \quad \text{(II-3)}$$

where $\alpha_1 = 1.08 \times 10^{-5}\ \mathrm{K}^{-1}$, $a = 2.81 \times 10^{-6}\ \mathrm{kg}^{-1}\ \mathrm{cm}^2$, $b = 5.78 \times 10^{-10}\ \mathrm{kg}^{-1}\ \mathrm{cm}^2\ \mathrm{K}^{-1}$, $c = 2.14 \times 10^{-11}\ \mathrm{kg}^{-2}\ \mathrm{cm}^4$, and $d = -4.58 \times 10^{-14}\ \mathrm{kg}^{-2}\ \mathrm{cm}^4\ \mathrm{K}^{-1}$.

III. Results

The actual data for each glass are in the form of the specific volume at 1 K intervals for 1 atm and 10 K intervals for elevated pressures. The thermal expansivities

Table I
Thermal Expansivity

P, kg cm^{-2}	0 glass		150 glass		300 glass		500 glass	
	$\alpha_0 \times 10^4$, K^{-1}	$\alpha_1 \times 10^7$, K^{-2}	$\alpha_0 \times 10^4$, K^{-1}	$\alpha_1 \times 10^7$, K^{-2}	$\alpha_0 \times 10^4$ K^{-1}	$\alpha_1 \times 10^7$, K^{-2}	$\alpha_0 \times 10^4$, K^{-1}	$\alpha_1 \times 10^7$, K^{-2}
1	1.370	1.779	0.662	4.168	0.653	4.200	0.805	3.484
100	1.303	1.884	0.790	3.530	0.890	3.095	1.003	2.650
200	1.388	1.390	1.173	2.037	1.116	2.130	1.072	2.226
300	1.339	1.423	1.382	1.190	1.148	1.811	1.132	1.870
400	1.087	2.023	1.073	2.047	1.201	1.494	1.100	1.798
500	1.034	2.037	1.334	1.011	1.226	1.247	1.165	1.396
600	0.966	2.084	1.128	1.497	1.200	1.165	1.210	1.045

Table II
Specific Volume at 290 K[a]

P, kg cm^{-2}	0 glass		150 glass		300 glass		500 glass	
	exptl	calcd[b]	exptl	calcd[b]	exptl	calcd[b]	exptl	calcd[b]
1	71325	71326	71288	71371	71244	71235	71166	71178
100	71161	71162	71128	71111	71092	71078	71009	71026
200	71010	71005	70975	70958	70940	70927	70859	70878
300	70856	70855	70826	70812	70798	70783	70714	70738
400	70709	70712	70683	70672	70657	70645	70577	70603
500	70567	70575	70547	70538	70523	70513	70447	70474
600	70422	70444	70416	70409	70394	70387	70323	70350

[a] $V \times 10^5$, cm^3 g^{-1}. [b] Calculated from eq VI-6 with eq VI-7.

α at 1 atm for the 150, 300, and 500 glasses are well represented by a linear expression in T:

$$\alpha = \alpha_0 + \alpha_1 T \qquad \text{(III-1)}$$

For 0 glass, the quadratic expression

$$\alpha = \alpha_0 + \alpha_1 T + \alpha_2 T^2 \qquad \text{(III-2)}$$

with $\alpha_0 = 1.370 \times 10^{-4}$ K^{-1}, $\alpha_1 = 3.159 \times 10^{-6}$ K^{-2}, and $\alpha_2 = 6.30 \times 10^{-9}$ K^{-3} is preferable in the temperature region 300–350 K. To facilitate the representation of the data and to put them into a more convenient form for our purpose, all the PVT data are contained in the values of the thermal expansivity expressed by eq III-1. The values of the constants α_0 and α_1 determined by least-squares are listed in Table I and the reference volumes at 290 K are given in Table II. The average standard deviation in the volume is 2.4×10^{-5} cm^3 g^{-1} at 1 atm and 6.5×10^{-5} cm^3 g^{-1} at elevated pressures. When errors due to systematic uncertainties in diameter of the mercury column, mass of the sample, pressure, and temperature are combined, the total experimental error in the volume is approximately $\pm 5 \times 10^{-5}$ cm^3 g^{-1} at 1 atm and $\pm 9 \times 10^{-5}$ cm^3 g^{-1} at elevated pressures.

The volume of each glass deviates slightly from that calculated from eq III-1 below 243 K at 1 atm and below 250 K at 600 kg cm^{-2} dut to the β-relaxation process. The data in these regions are excluded from the following discussions.

At 20 °C under atmospheric conditions, the specific volume of 0 glass formed at a cooling rate of 0.24 K/min is 0.714 cm^3 g^{-1}, which is lower than the value of 0.718 cm^3 g^{-1} reported by Hellwege, Knappe, and Lehmann[27] and the values of 0.718 and 0.716 cm^3 g^{-1} reported by Hydemann and Guicking[4] for glasses formed at cooling rates of 0.42 and 0.12 K/min. The glass transition temperature, T_g, of 0 glass is found to be 79.5 °C, which is higher than the values 75 and 72 °C for the glasses reported by Hydemann and Guicking.[4] The extent of desification in 500 glass is about 0.2%, which is smaller than the value 0.3% in 400 glass reported by Hydemann and Guicking.[4] These discrepancies cannot at present be attributed to explicit causes. These might be due to differences in the preparations and the purifications or the crystallinity of the sample.

Table III
Tait Parameters

sample	B_0, kg cm^{-2}	B_1, kg cm^{-2} K^{-1}	B_2, kg cm^{-2} K^{-2}	$C_0 \times 10^2$	$C_1 \times 10^5$, K^{-1}
0 glass	−950	23.474	−0.04580	2.781	6.87
150 glass	292	14.240	−0.02811	2.781	6.87
300 glass	783	12.844	−0.02837	2.781	6.87
500 glass	1009	9.521	−0.01978	2.781	6.87

The Tait equation

$$V/V_0 = 1 - C \ln (1 + P/B) \qquad \text{(III-3)}$$

where V_0 is the specific volume at 1 atm and B and C are temperature-dependent constants, is suitable for smoothing the data and convenient for comparison with others. Simha et al.[28,29] have shown that C can be set as 0.0894, common to various polymer liquids and glasses, and B can be expressed by

$$B = b_1 \exp(-b_2 T) \qquad \text{(III-4)}$$

However, when eq III-3 with $C = 0.0894$ and eq III-4 are applied to the present data, the average standard deviation in the relative volume is 6.5×10^{-4}, which is much larger than the experimental error. Hence we have allowed the constants C and B to vary with temperature by using polynomials in T:

$$C = C_0 + C_1 T \qquad \text{(III-5)}$$

$$B = B_0 + B_1 T + B_2 T^2 \qquad \text{(III-6)}$$

Here a common value of C was used for all the glasses. The values of the constants C_0, C_1, B_0, B_1, and B_2 estimated by least-squares regression are listed in Table III. The overall deviation in the relative volume was 1.68×10^{-4}.

As shown in Figure 3, the V–P isotherms are well represented by the Tait equation. In this figure, the Tait equation with the parameters determined by Simha et al.[29] from the data by Hellwege et al.[27] is also compared. At 600 kg cm^{-2}, the deviation is about 5×10^{-4} cm^3 g^{-1}, which is comparable to the experimental error in Hellwege et

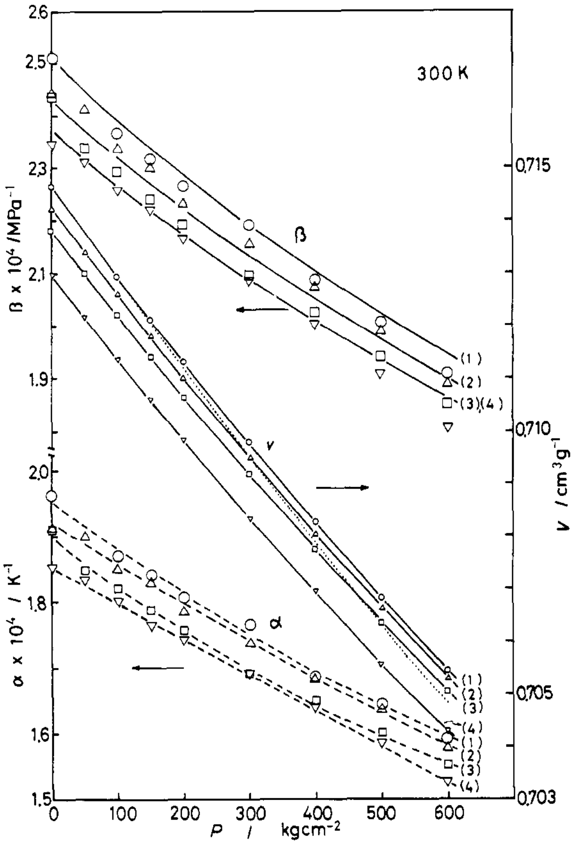

Figure 3. Isothermal variations of specific volume, thermal expansivity, and compressibility: (○) 0 glass; (△) 150 glass; (□) 300 glass; (▽) 500 glass. Solid lines, Tait equation; dotted line, Tait equation obtained by Simha et al;[29] broken lines, quadratic equations for α obtained by least-squares.

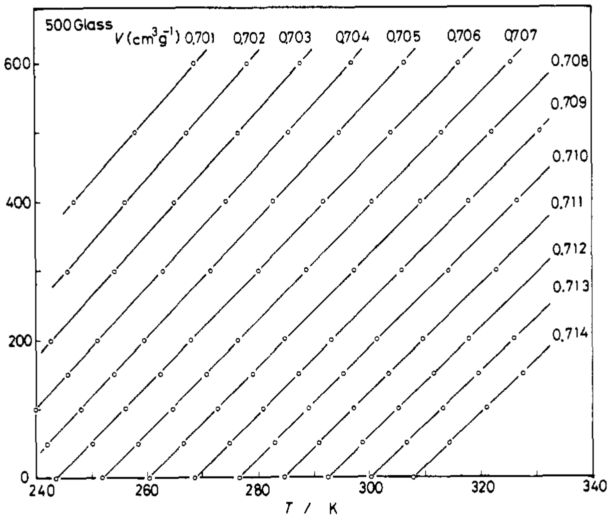

Figure 4. P–T isochores of 500 glass.

al.'s[27] data. The Tait equation is essentially empirical and used only for the data representation. We made no attempt in this paper to discuss the equation.

The thermal pressure coefficient γ was determined from the slopes of P–T isochores, which were approximately linear for all of the glasses over our experimental range, as shown, for example, in Figure 4. Thus in the glasses as well as in most liquids,[30] γ is approximated as a function of volume only. From the thermodynamic relation

$$[\partial(\partial S/\partial V)_T/\partial T]_V = [\partial(\partial E/\partial V)_T/\partial T]_V = 0 \qquad \text{(III-7)}$$

this leads to expressions in which the internal pressure, P_i, also is approximated as a function of volume only and in which the internal energy E and the entropy S are regarded as a simple sum of a term independent of volume and a volume-dependent term. This may offer a way to experimentally corroborate the postulate in the statistical model for the glass which leads to a partition function constituted by independent factors such as intramolecular kinetic terms and an intermolecular configurational term as well as in most statistical models[19,20,31-34] used to treat thermodynamic properties of polymer liquids and solutions.

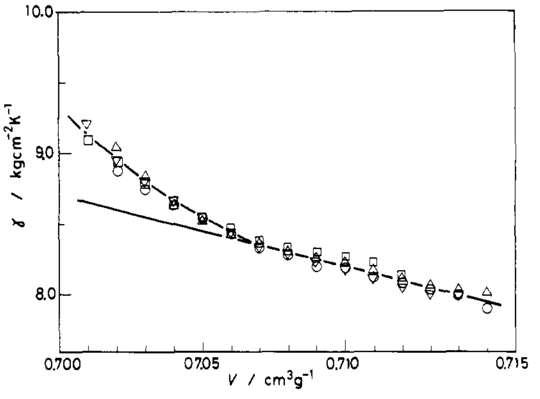

Figure 5. Thermal pressure coefficient as a function of volume: (○) 0 glass; (△) 150 glass; (□) 300 glass; (▽) 500 glass. Lines, eq III-8.

Figure 5 shows γ as a function of volume. γ for all of the glasses increases as the volume decreases. Effects of the glass-forming pressure on γ are not appreciable. The scatter in γ may be considered to be due to experimental error in regulation of pressure and cooling rate when the glasses were formed. Then we express the average values of γ as

$$\gamma = -4.89V + 4.27 \text{ MPa K}^{-1} \quad (V \geq 0.707) \qquad \text{(III-8a)}$$

$$\gamma = 862.29V^2 - 1226.76V + 437.12 \text{ MPa K}^{-1} \quad (V < 0.707) \qquad \text{(III-8b)}$$

Figure 3 shows the compressibility β obtained from $\beta = \alpha/\gamma$ with eq III-8 and III-1 and a comparison with those calculated from the Tait equation, eq III-3, with eq III-5 and III-6. The agreement is good.

As can be seen in Figure 3, the thermal expansivity and the compressibility depend on the glass-forming pressure. They decrease as the glass-forming pressure increases.

IV. Principle of Corresponding States

The principle of corresponding states for the equation of state is represented with reduced quantities (with tilde) by

$$f(\tilde{P},\tilde{V},\tilde{T}) = 0 \qquad \text{(IV-1)}$$

According to the corresponding states theory for polymer liquids developed by Hijimans,[35] the configurational quantities defined experimentally in the preceding section are related to the reduced quantities through characteristic reduction parameters (with asterisk):[36]

$$V = \tilde{V}V^* \quad E = \tilde{E}E^* \quad S = \tilde{S}S^* \quad T = \tilde{T}T^* \quad P = \tilde{P}P^* \qquad \text{(IV-2)}$$

$$P^* = E^*/V^* \qquad T^* = E^*/S^* \qquad \text{(IV-3)}$$

Some attempts to apply the principle of corresponding states to chemically different polymer glasses have been proposed by Simha and collaborators. Nanda and Simha[28] showed that the characteristic reduction parameters of

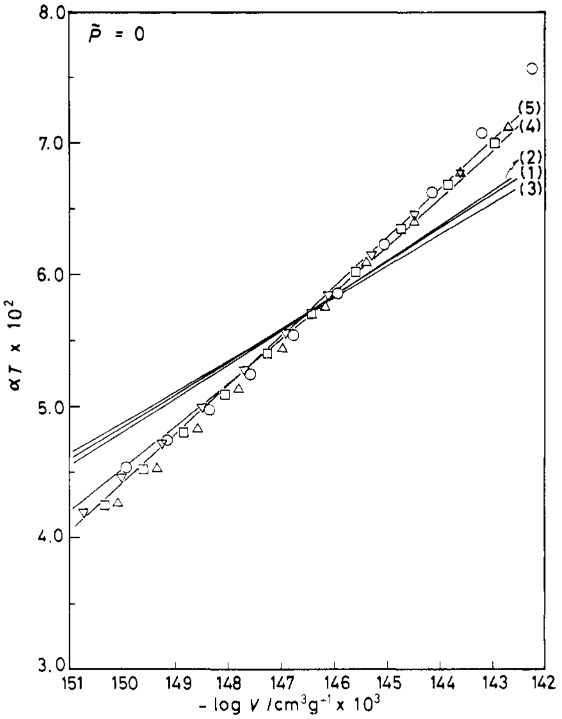

Figure 6. αT at zero pressure as a function of volume: (○) 0 glass; (△) 150 glass; (□) 300 glass; (▽) 500 glass; lines, theory. (1) Eq V-1; (2) eq V-2; (3) eq V-3; (4) eq VI-6 with $m_1 = 0$; (5) eq VI-6 with $m_0 = 0$.

PVC, polystyrene, and poly(methyl methacrylate) determined in the liquid range led to an approximately universal $\tilde{B}$–$\tilde{V}$ function, where the reduced Tait parameter $\tilde{B}$ equals B/P^*. However, no single universal function for $\tilde{V}$–$\tilde{T}$ relations was found.[37]

As a first step to examine the applicability of the principle of corresponding states to polymer glasses, we apply the principle to the densified glasses of PVC and attempt to elucidate the effect of the glass-forming history on the characteristic reduction parameters.

The ratio of the characteristic parameters of the densified glasses to those of 0 glass (as a reference) can easily be determined from a superposition method given by Nose et al.[38] Equations IV-1 and IV-2 lead to

$$\alpha T = (\partial \ln \tilde{V}/\partial \ln \tilde{T})_{\tilde{P}} \qquad \text{(IV-4)}$$

$$\beta P^* = -(\partial \ln \tilde{V}/\partial \tilde{P})_{\tilde{T}} \qquad \text{(IV-5)}$$

and, if the principle of corresponding states is applicable, αT and βP^* should be universal functions of the reduced quantities. At zero pressure, therefore, the experimental αT vs. log V plots for each glass would be shifted parallel to the log V axis to fall on a single master curve. Similarly, the superposition of the αT vs. log T plots parallel to the log T axis would give a second master curve. When $\tilde{T}$ obtained above is employed, the superposition of the log β vs. log $\tilde{T}$ plots parallel to the log β axis would give a third master curve. The shift factors obtained by the superpositions above are

$$\begin{aligned} a_i^V &= V_i^*/V_0^* \qquad a_i^T = T_i^*/T_0^* \\ a_i^P &= P_i^*/P_0^* \qquad (i = 1, 2, 3) \end{aligned} \qquad \text{(IV-6)}$$

where subscripts 0, 1, 2, and 3 are used to denote 0, 150, 300, and 500 glass, respectively. Equations IV-6 and IV-3 lead to[38]

$$\begin{aligned} a_i^E &= E_i^*/E_0^* = a_i^P a_i^V \\ a_i^S &= S_i^*/S_0^* = a_i^P a_i^V/a_i^T \qquad (i = 1, 2, 3) \end{aligned} \qquad \text{(IV-7)}$$

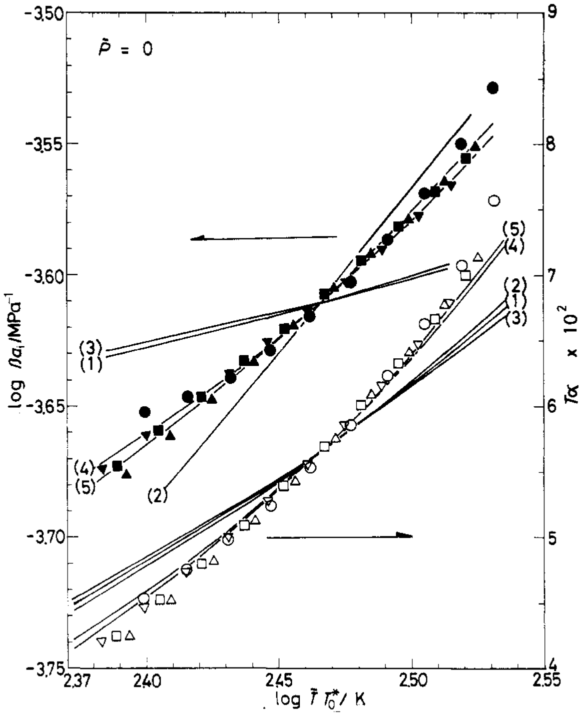

Figure 7. Master curves of αT and βa_i at zero pressure as a function of temperature. Symbols are the same as those in Figure 6.

Table IV
Ratios of Characteristic Parameters

sample	a^V, a^S	a^T, a^P, a^E
0 glass	1.000	1.000
150 glass	1.000	1.014
300 glass	1.000	1.023
500 glass	1.000	1.039

Figure 6 shows the experimental αT vs. log V plots at zero pressure, where α at zero pressure was obtained from extrapolations of the α vs. P curves approximated by the quadratic equations in P shown by the broken lines in Figure 3. As can be seen in Figure 6, αT values for various glasses, within experimental error, fall on a curve with no shift along the log V axis. Thus we obtain

$$a_i^V \simeq 1 \qquad V_0^* \simeq V_i^* \qquad (i = 1, 2, 3) \qquad \text{(IV-8)}$$

As shown in the preceding section, the thermal pressure coefficient γ can be approximated to be independent of the glass-forming pressure. Since the reduced thermal pressure coefficient is expressed as[38]

$$\tilde{\gamma} = \gamma(a_i^T/a_i^P)(T_0^*/P_0^*) \qquad \text{(IV-9)}$$

we obtain from eq IV-8 that the shift factor of the characteristic temperature is equal to that of the characteristic pressure:

$$a_i^T \simeq a_i^P \equiv a_i \qquad \text{(IV-10)}$$

From eq IV-7 and IV-10, the shift factors of the characteristic internal energy and entropy are equal to a_i and unity, respectively.

The master curve of the αT vs. log $\tilde{T}T_0^*$ plots obtained from the superpositions along the log T axis is shown in Figure 7, and the values of the resulting a_i are listed in Table IV. By using the a_i, we plot in Figure 7 log βa_i against log $\tilde{T}T_0^*$, where β at zero pressure was obtained from $\beta = \alpha/\gamma$ with eq III-8 and α at zero pressure. The log βa_i values fall on a master curve within experimental error.

Table V
Characteristic Parameters for 0 Glass

theory	eq	V^*, cm³ g⁻¹	T^*, K	P^*, MPa	y	k_g	m_0	m_1
Prigogine	V-1	0.6754	6302	656.6				
Flory	V-2	0.6765	17579	256.1				
Nose	V-3	0.632	10894	1139.5	1.1645			
this work	VI-6	0.6621	3033.9	388.78		1.045	0.6	0.0
	VI-6	0.6637	3337.3	425.99		1.045	0.0	0.6

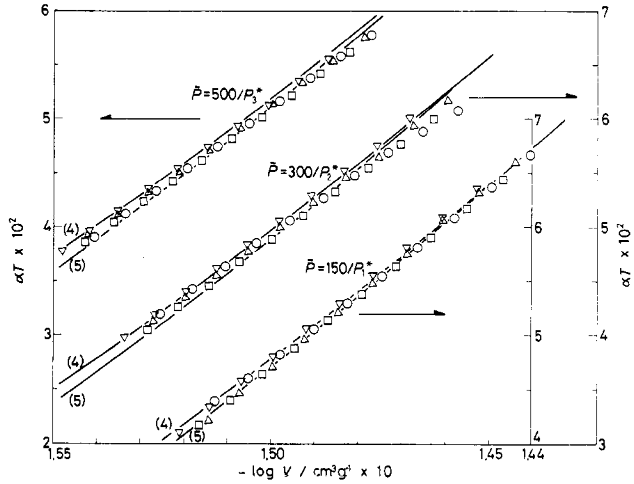

Figure 8. αT at higher pressures as a function of volume. Symbols are the same as those in Figure 6.

Thus the dependences of all the characteristic parameters on the glass-forming pressure are given at zero pressure. To ensure the applicability of the principle of corresponding states, αT at higher pressures, for example, are plotted against log V in Figure 8. At any pressure, αT can be regarded to fall on a master curve, within experimental error, with no shift along the log V axis.

According to Prigogine's theory,[19] the characteristic parameters are related to the molecular parameters as follows:

$$T^* = qz\epsilon^*/2ck \qquad P^* = qz\epsilon^*/2v^* \qquad V^* = Nv^* \tag{IV-11}$$

where qz is the effective coordination number per segment, $3c$ the number of external degrees of freedom per segment, ϵ^* the lattice energy parameter per cell, v^* the core volume of the segment, and N the segment number. From the superpositions above, it becomes evident that $qz\epsilon^*$ depends on the glass-forming pressure but not on c and v^*. That is, the potential energy factor only, and not the volume and entropy factors, is affected by the pressure history when the glass is isobarically formed at a constant cooling rate.

V. Applications of Some Equations of State

Since the Lennard-Jones and Devonshire cell model[39] was shown to apply well to the solid state,[40] the lattice-like theories for polymer liquids might be anticipated to apply to polymer glasses. Prigogine, Trappeniers, and Mathot derived an equation of state for polymer liquids from cell theory, with additional assumptions arising from the chainlike nature of the constituent molecules.[19] Its simplest form, with a square-well approximation by Nanda and Simha,[20] is expressed as[41]

$$\tilde{P}\tilde{V}/\tilde{T} = (1 - 2^{-1/6}\tilde{V}^{-1/3})^{-1} + 4(\tilde{V}^{-4} - \tilde{V}^{-2})/\tilde{T} \tag{V-1}$$

Using a van der Waals type intermolecular potential, Flory, Orwoll, and Vrij presented an equation of state:[31]

$$\tilde{P}\tilde{V}/\tilde{T} = (1 - \tilde{V}^{-1/3})^{-1} - \tilde{V}^{-1}/\tilde{T} \tag{V-2}$$

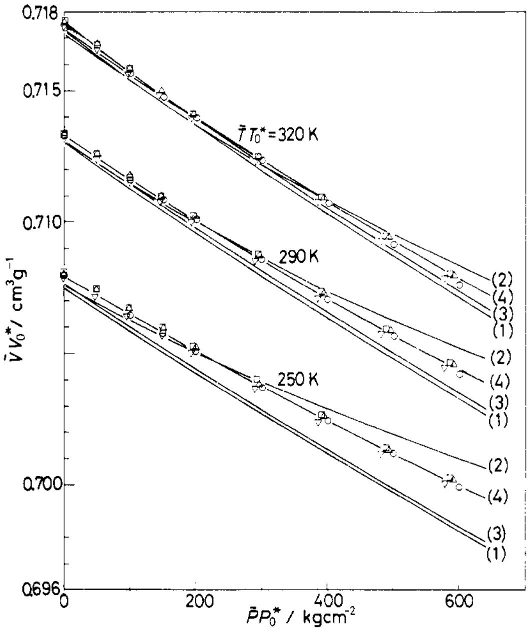

Figure 9. Master curves of specific volume as a function of pressure. Symbols are the same as those in Figure 6.

From hole theory, Simha and Somcynsky[32] and Nose[33] derived equations of state for polymer liquids. Incorporating the frozen-in holes in their theory, they proposed equations of state for glasses. Nose's equation,[18] which is essentially equivalent to that by Somcynsky and Simha,[17] is expressed as

$$\tilde{P}\tilde{V}(y - 1/6)6/5\tilde{T} = (y - 1/6)6/5 + 2^{-1/6}y^{1/3}\tilde{V}^{-1/3}/(1 - 2^{-1/6}y^{1/3}\tilde{V}^{-1/3}) + (2Ay^4\tilde{V}^{-4} - By^2\tilde{V}^{-2})/\tilde{T} \tag{V-3}$$

where $A = 1.0109$, $B = 2.4090$, and y is the fraction of occupies sites. Quach and Simha have shown that a constant condition of y with the reduction parameters determined in the liquid range underevaluates the thermal expansivity of the glass.[21] Here we examine this condition with reduction parameters obtained in the glassy states.

The characteristic parameters V^*, T^*, and P^* can easily be obtained by shifting the theoretical curves parallel to each log V, log T, and log β axis to give the best coincidence with the experimental master curves of αT and log βa_i in Figures 6 and 7. In Nose's equation, V^* was chosen from $V_0 = (2A/B)^{1/2}V^*$, where the liquid volume V_0 at 0 K was estimated from the group volume increments quoted by Bondi.[42] Then y was determined as an adjustable parameter by the superposition. Results are summarized in Table V.

As shown in Figures 6 and 7, the variations of αT and log β with V and T are not satisfactorily described by eq V-1 to V-3. This departure can more clearly be seen in the V–P isotherms in Figure 9. We conclude that eq V-1 to V-3 are not adequate for representation of the PVT relations of the present system.

Figure 10 shows the internal pressure calculated from $T\gamma - P$ with eq III-8 as a function of volume. Equations V-1 and V-3 are in excellent agreement with the experi-

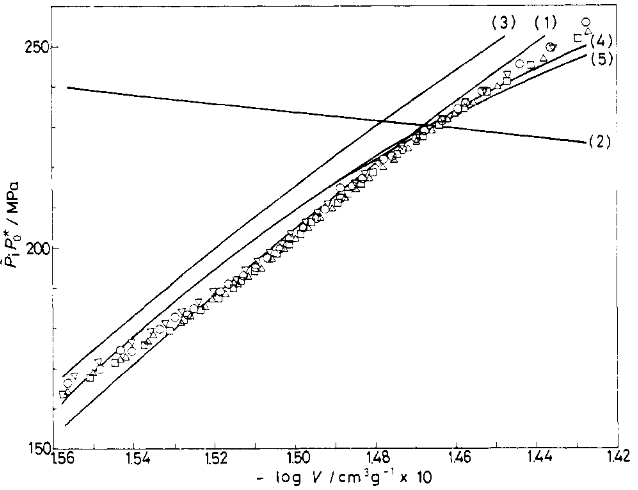

Figure 10. Internal pressure as a function of volume. Symbols are the same as those in Figure 6.

ments, but eq V-2 is not. For the glasses, therefore, the Lennard-Jones type lattice energy may be superior to the van der Waals type. The internal pressure is proportional to V^{-2} in the lattice–fluid theory of Sanchez and Lacombe[34] as well as in Flory's theory. Therefore, the former also may be inadequate for the glasses.

A discordance at the molecular level between theory and experiment is observed in the values of V^*. The values of V^* in eq V-1 and V-2 are much larger than that from the molecular model ($V^* \sim 0.63$ cm^3 g^{-1}) and are very close to the value of the specific volume of the glass at higher pressure. y in eq V-3 should be smaller than unity. Such a discordance is also observed in the analysis of the PVT relations of PVAc glasses[12] by McKinney and Simha,[22] who applied the Somcynsky–Simha theory[17] with the characteristic parameters determined in the liquid state, i.e., $y \sim 0.92$ and $V^* = 0.8141$. The value of V^* is equal to that of the specific volume of 0 glass at −30 °C and 700 bars and that of 800 glass at −30 °C and 450 bars.

These disagreements between theory and experiment are apparently due to the following peculiar properties of the glasses: notwithstanding that the volume is as large as that of the liquid, α and β are much smaller than those of the liquid, whereas variations of α and β with T and P are relatively large.

Cell theories, as pointed out by Kirkwood,[43] disregard local density and thermal potential energy fluctuations. In the liquid state, the time scale of the fluctuations is much faster than the experimental time scale. However, since the glass is formed on a time scale faster than the time required for regression of the local density fluctuations, the fluctuations near T_g may be frozen-in in the glassy state. Therefore, the assumptions involved in the cell theories might be of much greater importance in the glassy state than in the liquid state. On account of the frozen-in local density fluctuations, a permanent distribution of cell size may exist in the glassy state. This concept has already been inferred by McKinney and Simha from a study on the hole theory.[22] This concept seems to be also consistent with the argument for the β-relaxation process proposed by Johari and Goldstein.[44] We will attempt to modify Prigogine's theory in a simplified manner and to compare it with experiment in the next section.

VI. Frozen-In Cell Model

Theory. Although a long-range cooperative rearrangement is forbidden in the glassy state, some of the segments which are contained in the cells of larger size may retain the local external degrees of freedom. These segments may predominantly contribute to the configurational properties of the glass.

We assume that M cells are so small that the segments in the cells are observed to be apparently frozen-in. Further, we shall assume the M cells to be of uniform size v_g^* and the $N - M$ cells also to be of uniform size. Then the average nearest-neighbor distance of the segments in the $N - M$ cells is expressed by

$$a = [2^{1/2}(Nv - Mv_g^*)/(N - M)]^{1/3} \qquad \text{(VI-1)}$$

where hexagonal packing is assumed.

The number of frozen-in cells, M, may depend on the fluctuation at T_g. Since the variation of the glass transition temperature with pressure is in close agreement with that obtained from dielectric time–temperature superposition in the liquid state,[14-16] the present glasses are considered to be formed at an isorelaxation time. Therefore, M may be regarded to be independent of the glass-forming pressure.

When the frozen-in parameters k_g and m are defined by

$$k_g = v_g^*/v^* \qquad m = M/N \qquad \text{(VI-2)}$$

eq VI-1 is expressed as

$$a = (2^{1/2}\tilde{v}'v^*)^{1/3} \qquad \text{(VI-1')}$$

where

$$\tilde{v}' = (\tilde{v} - mk_g)/(1 - m) \qquad \text{(VI-3)}$$

Then the free volume is given by

$$v_f = (2^{1/6}\tilde{v}'^{1/3} - 1)^3 v^* \qquad \text{(VI-4)}$$

Following Prigogine's theory[19] with the square-well potential approximation,[20] we assume the reduced partition function to take the form

$$Z = v_f^{c(N-M)} \exp[-(N - M)zq\epsilon^*(A\tilde{v}'^{-4} - B\tilde{v}'^{-2})/2kT] \qquad \text{(VI-5)}$$

Then we have the reduced equation of state

$$\tilde{P}\tilde{V}/\tilde{T} = K[(1 - 2^{-1/6}\tilde{V}'^{-1/3})^{-1} + (2A\tilde{V}'^{-4} - B\tilde{V}'^{-2})2/\tilde{T}] \qquad \text{(VI-6)}$$

where

$$K = \tilde{V}\tilde{V}'^{-1} \qquad \text{(VI-7)}$$

and the characteristic parameters T^*, P^*, and V^* are given by eq IV-11.

A cell of a size slightly larger than v_g^* might be frozen-in when the temperature is lowered or the pressure is increased. Assuming this contribution to be approximated by

$$m = m_0 + m_1\tilde{v}^{-1} \qquad \text{(VI-8)}$$

we have the front factor K in eq VI-6 as

$$K = \tilde{V}\tilde{V}'^{-1} - m_1\tilde{V}^{-1}(1 - k_g\tilde{V}'^{-1}) \qquad \text{(VI-7')}$$

Now we have an equation of state, eq VI-6, with T^*, P^*, V^*, and two (m_0, k_g) or three (m_0, m_1, k_g) additional parameters.

Comparison with Experiments. Comparisons between theory and experiment are made with respect to the two cases of $m_1 = 0$ and $m_0 = 0$. V^*, T^*, P^*, k_g, and m_0 or m_1 were determined according to the procedure outlined below. First m_0 (m_1) was changed in increments of 0.1 over the range 0–1, with k_g being fixed at unity. For each value of m_0 (m_1), the theoretical curve was shifted to give a coincidence with the experimental master curves of αT and

$\log \beta a_i$ at zero pressure (Figures 6 and 7), and the value of m_0 (m_1) which gave the best coincidence was found to be 0.6. Then k_g was changed in increments of 0.001 with m_0 (m_1) held fixed at 0.6, and the value of k_g which gave the best coincidence with the experiments was determined to be 1.045. Furthermore, m_0 (m_1) was changed in increments of 0.1 with the value of k_g fixed at 1.045; we again obtained m_0 (m_1) = 0.6. The thus-obtained values are listed in Table V. The results are compared with the experiments in Figures 8–10 and Table II.

The theoretical equation of state with the parameters at zero pressure is in satisfactory agreement with the experimental thermal expansivity at higher pressures (Figure 8), V–P isotherms (Figure 9 and Table II), and internal pressure (Figure 10). In the regions above 310 and below 270 K, eq VI-6 rather than the Tait equation, eq III-3 with eq III-5 and III-6, agrees with the experimental V–P isotherms.

As can be seen in Figures 6–8 and 10, the correction factor m_1 in eq VI-8 is not particularly necessary in the present temperature and pressure range. Such a correction, even if introduced, would probably exert only a slight effect since the theory includes the drastic assumption of the separation of uniform-sized cells into ones with $v = v_g^*$ and others with $v > v_g^*$.

The value of V^* is equal to 0.662 cm^3 g^{-1}, which is smaller than those in eq V-1 and V-3 but larger than the value of 0.632 cm^3 g^{-1} from the molecular model. This may indicate a discordance at the molecular level between theory and experiment. The fact that the value of m is 0.6 apparently indicates that about 60% of the segments are frozen-in in the glassy state. However, this percentage, although it seems not to be very improper, should not be of much importance because of the reason mentioned above.

VII. Conclusion

There have been many discussions on the glass and the glass transition in terms of one or two frozen-in configurational parameters in the liquid state, such as free volume and/or configurational entropy.[17,18,44] Differing from such traditional models, the present study offers an analysis of the glassy state apart from the liquid characteristics. This is because, despite the extensive investigations, the explicit mechanism and the criterion of the glass transition still seem to be obscure. Recently, from detailed analyses of the specific heat and its increment at the glass transition temperature, Goldstein[46] and Roe and Tonelli[47] argued that the glass transition is accompanied by additional effects, such as changes in the vibrational frequencies or in other modes of thermal excitation. This conclusion, if true, suggests that the traditional models are not appropriate.

The representation of the PVT data based on the principle of corresponding states is independent of models for the glass. The conditions for the existence of the principle do not depend on the functional form of the equation of state but do depend on a universality of the intermolecular force law.[35] This universality may be expected for glasses of a single substance formed at pressures lower than the internal pressure.

The results of the analysis in terms of the principle of corresponding states indicate that the effective coordination number and/or the intermolecular force constant varies with the glass-forming pressure. That is, the segments of the glass formed at higher pressure are confined within the cells with higher potential energy. Thus its thermal expansivity is smaller than that of the glass formed at lower pressure. The results indicate also that the core volume and the entropy factor are not altered by the glass-forming pressure. This may lead to the mobile unit of the molecular motions being independent of the pressure history. Thus the presented results suggest that the energy field may play an important role in the molecular motions in the glassy state.

The configurational properties of the glass may occur from the localized mode of motions governed by the localized energy field since long-range cooperative rearrangements are forbidden in the glassy state. In other words, there may exist a range of frozen-in cells which participate only slightly in the external molecular motions and the configurational properties of the glass. This seems to be the essential reason that the theories for polymer liquids have failed to represent the PVT data of the glass.

The inclusion of the distribution of cell size in the cell theory in the simplest manner gives a satisfactory agreement with experiment. However, we remark that the present theory contains two supplemental adjustable parameters in addition to the characteristic parameters. Therefore, the agreement may not directly demonstrate the validity of the present model.

Acknowledgment. We thank Professor Shigeyuki Ueda of this laboratory for his interest in this work and the encouragement he provided.

References and Notes

(1) Tammann, G.; Jenckel, E. *Z. Anorg. Allg. Chem.* **1929**, *184*, 416.

(2) Shishkin, N. I. *Sov. Phys.—Solid State* (*Engl. Transl.*) **1960**, *2*, 322. Shishkin, N. I.; Kovalichev, O. F. *Ibid.* **1960**, *2*, 329.

(3) The densifications of inorganic oxide glasses are reviewed in: Sakka, S.; MacKenjie, J. D. *J. Non-Cryst. Solids* **1969**, *1*, 107.

(4) Heydemann, P.; Guicking, H. D. *Kolloid Z. Z. Polym.* **1963**, *193*, 16.

(5) Gee, G. *Polymer* **1966**, *7*, 177.

(6) Rehage, G.; Breuer, H. *J. Polym. Sci., Part C* **1967**, *16*, 2299.

(7) Bianchi, U.; Turturro, A.; Basile, G. *J. Phys. Chem.* **1967**, *71*, 3666.

(8) Allen, G.; Ayerst, R. C.; Cleveland, J. R.; Gee, G.; Price, C. *J. Polym. Sci., Part C* **1968**, *23*, 127.

(9) Kimmel, R. M.; Uhlmann, D. R. *J. Appl. Phys.* **1970**, *41*, 2917.

(10) Ichihara, S.; Komatsu, A.; Tsujita, Y.; Nose, T.; Hata, T. *Polym. J.* **1971**, *2*, 530. Ichihara, S.; Komatsu, A.; Hata, T. *Ibid.* **1971**, *2*, 644, 650.

(11) Weitz, A.; Wunderlich, B. *J. Polym. Sci., Polym. Phys. Ed.* **1974**, *12*, 2473.

(12) McKinney, J. E.; Goldstein, M. *J. Res. Natl. Bur. Stand., Sect. A* **1974**, *78*, 331.

(13) Price, C. *Polymer* **1975**, *16*, 585.

(14) O'Reilly, J. M. *J. Polym. Sci.* **1962**, *57*, 429.

(15) Goldstein, M. *J. Phys. Chem.* **1973**, *77*, 667.

(16) Miller, A. A. *Macromolecules* **1978**, *11*, 134.

(17) Somcynsky, T.; Simha, R. *J. Appl. Phys.* **1971**, *42*, 4545.

(18) Nose, T. *Polym. J.* **1971**, *2*, 427.

(19) Prigogine, I.; Trappeniers, N.; Mathot, V. *Discuss. Faraday Soc.* **1953**, *15*, 93.

(20) Nanda, V. S.; Simha, R. *J. Phys. Chem.* **1964**, *68*, 3158.

(21) Quach, A.; Simha, R. *J. Phys. Chem.* **1972**, *76*, 416.

(22) McKinney, J. E.; Simha, R. *Macromolecules* **1974**, *7*, 894. *Ibid.* **1976**, *9*, 430.

(23) For instance: D'Amato, R. J.; Strella, S. *Appl. Polym. Symp.* **1969**, *8*, 275. Nakajima, A.; Hamada, H.; Hayashi, S. *Makromol. Chem.* **1966**, *95*, 40.

(24) (a) Wendorff, J. H.; Fischer, E. W. *Kolloid Z. Z. Polym.* **1973**, *251*, 884. (b) Neilson, G. F.; Jabarin, S. A. *J. Appl. Phys.* **1975**, *46*, 1175. (c) Straff, R. S.; Uhlmann, D. R. *J. Polym. Sci., Polym. Phys. Ed.* **1976**, *14*, 353. (d) Geil, P. H. *J. Macromol. Sci., Phys.* **1977**, *14*, 171. (e) Blundell, D. J. *Polymer* **1979**, *20*, 934.

(25) Pigg, P. H. *Br. J. Appl. Phys.* **1964**, *15*, 1111.

(26) Davis, L. A.; Gordon, R. B. *J. Chem. Phys.* **1967**, *46*, 2650.

(27) Hellwege, K. H.; Knappe, W.; Lehmann, P. *Kolloid Z. Z. Polym.* **1963**, *183*, 110.

(28) Nanda, V. S.; Simha, R. *J. Chem. Phys.* **1964**, *41*, 3870. Quach, A.; Simha, R. *J. Appl. Phys.* **1971**, *42*, 4592.

(29) Simha, R.; Wilson, P. S.; Olabisi, O. *Kolloid Z. Z. Polym.* **1973**, *251*, 402.

(30) For instance: Rowlinson, J. S. "Liquids and Liquid Mixtures", 2nd ed.; Butterworths: London, 1971.
(31) Flory, P. J.; Orwoll, R. A.; Vrij, A. *J. Am. Chem. Soc.* **1964**, *86*, 3507, 3515.
(32) Simha, R.; Somcynsky, T. *Macromolecules* **1969**, *2*, 342.
(33) Nose, T. *Polym. J.* **1971**, *2*, 124.
(34) Sanchez, I. C.; Lacombe, R. H. *J. Phys. Chem.* **1976**, *80*, 2352.
(35) Hijimans, J. *Physica (Utrecht)* **1961**, *27*, 433.
(36) Bhattacharyya, S. N.; Patterson, D.; Somcynsky, I. *Physica (Utrecht)* **1964**, *30*, 1276.
(37) Nanda, V. S.; Simha, R.; Somcynsky, T. *J. Polym. Sci., Part C* **1966**, *12*, 277.
(38) Kusuhara, Y.; Nose, T.; Hata, T. *Rep. Prog. Polym. Phys. Jpn.* **1971**, *14*, 301. Noguchi, H.; Nose, T. *Kobunshi Ronbunshu* **1976**, *33*, 293.
(39) Lennard-Jones, J. E.; Devonshire, A. E. *Proc. R. Soc. London, Ser. A* **1937**, *163*, 53. *Ibid.* **1938**, *165*, 1.
(40) Barker, J. A. "Lattice Theories of the Liquid State"; Pergamon Press: New York, 1963.
(41) Patterson, D.; Bhattacharyya, S. N.; Picker, P. *Trans. Faraday Soc.* **1968**, *64*, 648.
(42) Bondi, A. "Physical Properties of Molecular Crystals, Liquids, and Glasses"; Wiley: New York, 1968; Chapter 14.
(43) Kirkwood, J. G. *J. Chem. Phys.* **1950**, *18*, 380.
(44) Johari, J. P.; Goldstein, M. *J. Chem. Phys.* **1970**, *53*, 2372. *Ibid.* **1971**, *55*, 4245.
(45) For instance: Gibbs, J. H.; DiMarzio, E. A. *J. Chem. Phys.* **1958**, *28*, 373.
(46) Goldstein, M. *J. Chem. Phys.* **1976**, *64*, 4767. *Ibid.* **1977**, *67*, 2246.
(47) Roe, R. J.; Tonelli, A. E. *Macromolecules* **1978**, *11*, 114.

Self-Consistent Field Conformational Energy Calculations for *n*-Alkanes and Characterizations of Polymethylene

J. A. Darsey*

Department of Chemistry, Louisiana State University, Baton Rouge, Louisiana 70803

B. K. Rao

Institute of Physics, A-105 Saheed Nagar, Bhubaneswar-751007, Orissa, India.

Received November 21, 1980

ABSTRACT: Self-consistent field molecular orbital (SCF–MO) methods have been used to determine the energies of *n*-butane and *n*-pentane in various conformations. Complete geometry optimization was employed to obtain the best minimum energy at the trans and various gauche conformations. The values of E_σ and E_ω thus obtained were 1191 and 1930 cal/mol, respectively. The position and magnitude of the rotational potential barrier were found to be $\phi_2 = 60°$ and 3.7 kcal/mol, respectively. The latter is to be compared with the experimental value of 3.3–3.7 kcal/mol. E_σ and E_ω at 140 °C were used in calculating the rotational isomeric state (RIS) statistical parameters $\sigma = 0.23$ and $\omega = 0.095$. The principal advantage of using SCF–MO ab initio methods to calculate the conformational energies is that no arbitrary parameters are required, as are required in semiempirical works.

I. Introduction

For many years, the statistical parameters used for *n*-alkanes and higher homologues have been calculated with semiempirical expressions[1-5] for the energy. In general, the energy has been considered to consist of three parts: (i) intrinsic torsional potentials, (ii) van der Waals repulsions between nonbonded atoms and groups, and (iii) dispersion attractions between nonbonded atoms. The torsional term is considered to be dependent upon the dihedral angles of internal rotation and on the choice of the fixed valence angles and is represented by an expression[4-7] of the form $^1/_2E_0(1 - \cos 3\phi)$, where E_0 is the height of the potential barrier against internal rotation and ϕ is the angle through which a rotation is made about any particular bond. The nonbonded interactions (ii) and (iii) are expressed as a Lennard-Jones 6–12 potential function of the form[3]

$$\sum_{k<l}(a_{kl}/r_{kl}^{12} - c_{kl}/r_{kl}^{6})$$

Flory and others[4,8] have also used a Buckingham potential where the repulsive r^{-12} part is replaced by an exponential term and is expressed as

$$\sum_{k<l}[a_{kl}\exp(-b_{kl}r_{kl}) - c_{kl}/r_{kl}^{6}]$$

In these expressions, r_{kl} is the internuclear distance between atoms k and l for a given conformation and a_{kl}, b_{kl}, and c_{kl} are constants independent of r_{kl}. The van der Waals constant, c_{kl}, can usually be obtained from many theoretical sources very accurately. One source used frequently is values calculated from the Slater–Kirkwood equation.[1] From these, one obtains the expression for the intramolecular energy[2-4,9] associated with a rotation through ϕ_i about the ith bond as

$$E(\phi_i) = {}^1\!/_2E_0(1 - \cos 3\phi_i) + \sum_{k<l}(a_{kl}/r_{kl}^{12} - c_{kl}/r_{kl}^{6}) \qquad (1)$$

or in an equivalent form using the Buckingham potential. While using these expressions, one adjusts the parameters a_{kl} and b_{kl} arbitrarily[4] so as to reproduce the observed energy difference between the gauche and trans conformations of the molecule under study. The calculated energies are then used to calculate statistical parameters incorporated into the rotational isomeric state (RIS) theory.[10-13]

Briefly, the rotational isomeric state theory states that the total conformational energy for a chain molecule can